

Arsenic and Antimony Removal from Water by Zirconium-Coated Water Treatment Plant Sludge

Berna KAVACIK^{1*}, Deniz DÖLGEN²

Abstract

In this study, the reuse potential of drinking water treatment sludge as an adsorbent was investigated for the removal of arsenic and antimony. A sludge-derived adsorbent, zirconium oxide-coated sludge, was produced by using thermal treatment and zirconium oxide coating processes, and characterization of the adsorbent was investigated. The results showed that zirconium oxide-coated sludge was mainly amorphous and had a high surface area ($170 \text{ m}^2\text{g}^{-1}$). Batch adsorption tests were performed to specify the optimum conditions for arsenic removal. The study revealed that the removal of As (T) was best achieved at pH 3. The initial arsenic concentration descended from $50 \text{ }\mu\text{gL}^{-1}$ to the $0.25 \text{ }\mu\text{gL}^{-1}$ at contact time, 180 min, with the adsorbent dose of 1 gL^{-1} . The isotherm data fitted fine to the Freundlich isotherm model, and adsorption capacity was found to be 7.38 mgg^{-1} . The pseudo-second order model fitted well with the experimental data ($R^2 \geq 0.999$). Column performance for arsenic and antimony removal in a fixed bed under continuous flow conditions was also studied. The adsorption process behavior was described successfully by Thomas and Yoon–Nelson models, indicating that the models were suitable for a zirconium oxide-coated sludge fix-bed column design.

Keywords: Adsorption, Antimony, Arsenic, Drinking water treatment sludge, Zirconium oxide coating

Zirkonyum Kaplı Su Arıtma Tesisi Çamurları ile Sudan Arsenik ve Antimon Giderimi

Öz

Bu çalışmada, arsenik ve antimon gideriminde içme suyu arıtma çamurlarının adsorban olarak yeniden kullanım potansiyeli araştırılmıştır. Zirkonyum oksit kaplı çamur termal arıtım ve zirkonyum oksit kaplama prosesleriyle üretilmiş ve adsorbanın karakterizasyonu araştırılmıştır. Sonuçlar, zirkonyum oksit kaplı çamurun ağırlıklı olarak amorf olduğu ve yüksek yüzey alanına ($170 \text{ m}^2\text{g}^{-1}$) sahip olduğunu göstermiştir. Arsenik gideriminde optimum koşulların belirlenmesi amacıyla kesikli adsorpsiyon deneyleri gerçekleştirilmiştir. Deney sonucunda optimum pH 3 olarak elde edilmiş, 1 gL^{-1} adsorban dozunda 180 dk. temas süresinde arsenik konsantrasyonu $50 \text{ }\mu\text{gL}^{-1}$ den $0.25 \text{ }\mu\text{gL}^{-1}$ 'ye düşmüştür. İzoterm verisi Freundlich izoterm modeline uyumu ve adsorpsiyon kapasitesi 7.38 mgg^{-1} olarak bulunmuştur. Deneysel verilerin yalancı ikinci derece kinetiğe uyum sağladığı ($R^2 \geq 0.999$) saptanmıştır. Ayrıca sürekli akış koşullarında sabit yataklı kolonda arsenik ve antimon gideriminin kolon performansı araştırılmıştır. Adsorpsiyon proses davranışının Thomas ve Yoon–Nelson modelleri tarafından başarıyla tanımlanması, modellerin sabit yataklı kolon dizaynında zirkonyum oksit kaplı çamur için uygun olduğunu göstermektedir.

Anahtar Kelimeler: Adsorpsiyon, Antimon, Arsenik, İçme suyu arıtma çamuru, Zirkonyum oksit kaplama

¹Dokuz Eylül University, Graduate School of Natural and Applied Sciences, Department of Environmental Engineering, Izmir, Turkey, berna_dalkiran@hotmail.com

²Dokuz Eylül University, Faculty of Engineering, Department of Environmental Engineering, Izmir, Turkey, deniz.dolgen@deu.edu.tr

¹<https://orcid.org/0000-0002-1756-8917> ²<https://orcid.org/0000-0002-5888-3032>

1. Introduction

Arsenic (As) and antimony (Sb) are harmful contaminants because they have high toxicity and are regarded to be environmental pollutants of global concern (Shtangeeva et al., 2011; Lee et al., 2018). Both As and Sb belong to the same periodic group and have shown similar chemical characteristics (Lan et al., 2016). Hence, chemical similarities between As and Sb are often discussed in order to transfer the knowledge from As to Sb (Kolbe et al., 2011). Antimony is typically found with arsenic in natural groundwater aquifers. They are introduced naturally into groundwater through the weathering reactions of geogenic mineral rocks and microbial activities as well as through anthropogenic facilities like industrial discharges, mining, and farming. Although behavior of As has been investigated heretofore, the transfer of Sb into the environment is not still adequately known, and this lack of knowledge has resulted in questionable conclusions.

Arsenic, a well-known carcinogen, is considered as one of the world's most hazardous chemicals and is currently regarded as a cause of major health problems in several regions of the world. The toxicity of antimony is also presumed to be similar to that of arsenic in respect to impacts and mechanism (Xi et al., 2010). Since both pollutants are toxic and carcinogenic, their mitigation from water is of unquestionable importance. An estimated 300 million people worldwide are affected by As poisoning leading to health hazards (Kumar et al., 2021). It is also estimated that nearly 108 countries are affected by As contamination in groundwater (Shaji et al., 2021). Turkey has recently been included in the list of countries where arsenic pollution poses increasing risk. Therefore, As pollution has become an important topic of consideration in Turkey as well (Dolgen et al., 2019). In addition to the elevated levels of As concentrations, the occurrence of Sb in groundwater has also received attention. It is speculated that Sb could be a natural co-contaminant with As in some drinking-water (WHO, 2003). The coexistence of toxic As and Sb poses difficulties for their simultaneous removal. Since most groundwater systems are considered an essential source for potable water in many settlements, implementation of the mitigation measures for both As and Sb is of vital importance. Wellhead treatment systems (mainly package water treatment plants) have been proposed as an appropriate solution, especially for small communities in remote areas. Among the wellhead treatment systems, adsorption, ion exchange, and filtration processes are prominent. Adsorption is proposed as an effective and easy to manage technology to eliminate these contaminants with low sludge production. The most important problem herein is to provide efficient and low-cost adsorbent.

Therefore, in the last several decades, because use of waste materials as adsorbents contributes to cost reduction for waste disposal, researchers have attempted to enhance adsorbents from them (Sasaki et al., 2014; Ocinski et al., 2016; Soleimanifar et al., 2016; Wang et al., 2018;

Tan et al., 2018). In this framework, the use of drinking water treatment sludge (DWTS) has gained popularity because of its eco-friendly advantages (both ecologic and economic). Although its' physical and chemical characteristics depend mainly upon the raw water quality, the chemicals used for treatment, and the operating conditions (Ippolito et al., 2011), addition of metal salts to the raw water is a common practice. The addition of aluminum (Al) or iron (Fe) salts results in the generation of Al or Fe hydroxides sludges; thus, drinking water plants residuals containing Al or Fe hydroxides exhibit greater capacity to purify arsenic and antimony from water. In the literature, adsorption of arsenic, phosphate, and sulphate by DWTS have been documented by various researchers, but there is no data on the efficacy of DWTS for antimony adsorption (Caporale et al., 2013; Nagar et al., 2010; Ocinski et al., 2016; Razali et al., 2007; Sun et al., 2015; Wang et al., 2018).

Additionally, various modifications have been sought in attempts to enhance the adsorption performance of the adsorbents. Metal oxides are preferred to modify adsorbents in order to increase their affinity for arsenic species in particular. The elements such as Al, Mn, Zn, Zr, etc. have been integrated with iron oxides to produce bimetal oxides to improve the performance of iron oxides for the adsorption of anions (Li et al., 2012; Lu et al., 2015; Masue et al., 2006; Zhang et al., 2007). Lu et al. (2015) studied simultaneous removal of arsenate and antimonate on Fe/Zn layered double hydroxide and achieved a relatively high adsorption capacity (i.e., 151 mgg⁻¹ and 122 mgg⁻¹ for As(V) and Sb(V), respectively). Among the various elements, zirconium oxide has drawn attention due to its high resistance to reductants, oxidants, alkalis, and acids. According to Li et al. (2012), the zirconium oxide adsorption capacity was higher than that of FeOOH. Ironzirconium bimetal oxide has also been studied for antimony (V) removal by them. Ironzirconium bimetal oxide displayed a superior performance for antimony removal than ferric oxide or zirconium oxide.

The main goals of the study were to develop a sludge-derived adsorbent, and use it for arsenic and antimony removals. Since high arsenic concentrations above the standard (i.e., 10 ppb) has been measured in various drinking water sources, it has been an important topic in the agenda of Turkey (Varol and Köse, 2018; Baba and Tayfur, 2011). In addition to the elevated levels of arsenic concentrations, the occurrence of antimony in ground water has also received attention in many places because of the coexistence of As and Sb poses difficulties for their simultaneous removal (Kolbe et al. 2011; Long et al., 2022). For this reason, we focused on the simultaneous treatment of arsenic and antimony in the study. Our principal hypothesis was sludge-derived materials containing high concentration of ferric ions which have a high affinity to As, can efficiently remove the As and Sb from water, as well. In this framework, batch experiments and column studies were conducted to assess the performance of the adsorbent zirconium oxide-coated sludge (ZOC-DWTS) for arsenic and antimony removal. The operational parameters like pH, adsorbent dose, contact

time, and initial solute concentration were investigated in batch experiments. Freundlich, Langmuir, and Temkin isotherms were studied to define the adsorption mechanisms. The kinetic parameters were calculated by fitting the various kinetic models (first order, second order, pseudo-first order, and pseudo-second order reaction models). Finally, the Yoon-Nelson and Thomas models were employed to predict the column performance and breakthrough curve. It was concluded that the column packed with ZOC-DWTS could be used effectively to treat arsenic and antimony contaminated water.

2. Materials and Methods

2.1. Preparation of the Adsorbent (ZOC-DWTS)

The DWTS sample containing a high quantity of iron was obtained from a drinking water treatment plant in Izmir, Turkey. This treatment plant consists of cascade aeration, chemical treatment, clarification, rapid sand filter, and disinfection units. Ferric chloride is used as a coagulant in the chemical treatment process, and thus sludge containing iron hydroxide is produced. Sludge is processed in thickener and dewatering units. Sludge samples having 30-35% solid content were taken from the outlet of the filter press unit. DWTS samples were air-dried, ground, and sieved to a diameter of 0.250 mm-2 mm. Then, they were washed with deionized water until the water was colorless and then dried at 105°C (Caporale et al., 2013; Wang et al., 2016; Wang et al., 2018). Sludge samples were then heated at temperatures of 200, 400, and 600°C in an oven for 1 and 4 h. Heating used in the experiments was principally based upon the methods identified in Chen et al. (2008) and Li et al. (2014). Because the most effective temperature was found to be 200°C, batch and column experiments were performed with 200°C heated sludge. Then, heated materials were washed with deionized water and were kept at 100°C in the oven. Following the thermal process, it was modified by zirconium oxide to exploit the synergetic effect of the presence of both metals. The zirconium coating was applied for modification taking the method reported by Chaudhry et al. (2017) into consideration. Briefly, a 125 mL 0.125 M $ZrOCl_2 \cdot 8H_2O$ solution was poured, and 25 g of DWTS was added to a beaker of 500 mL NaOH or HCl solutions were added to sustain the pH at about 7.5. The solution was mixed continuously for 22 hours. Afterwards, coated DWTS was held in solution for 3 h and then filtered. The ZOC-DWTS was kept at 105°C in an oven for 22 h and washed several times with pure water to eliminate slightly held oxide particles. Then, it was dried at 105°C in an oven for 3 h.

2.2. Adsorbate

All chemicals used in the experiments were reagent grade. A $1000\pm 6 \mu\text{g mL}^{-1}$ concentration of arsenic and a $1000\pm 4 \mu\text{g mL}^{-1}$ concentration of antimony stock solutions was used and preserved with 2% HNO_3 for arsenic and 5% HNO_3 +0.1% HF for antimony. Stock solutions were diluted by deionized water to obtain the desired arsenic and antimony concentrations used in the experiments.

Batch experiments were also performed with real groundwater obtained from the Bayındır-Dernekli well. Groundwater from the well contained arsenic (0.009 mg L^{-1}), antimony (0.056 mg L^{-1}), phosphate ($<0.4 \text{ mg L}^{-1}$), manganese (0.27 mg L^{-1}), and iron (0.3 mg L^{-1}) ions.

2.3. Adsorbent Characterization

In the experiments, the elemental composition of the materials was examined with an energy dispersing X-ray spectroscopy (EDS), and X-ray diffraction (XRD) analysis (phase analysis) was carried out to determine the crystal structure and assign the components. The surface morphologies of the adsorbent were analyzed by a scanning electron microscope (SEM). Pore volume and surface area of the materials were determined by the Brunauer, Emmet, and Teller (BET) analysis (Nekhunguni et al., 2017; Ocinski et al., 2016).

2.4. Arsenic and Antimony Measurements

Analysis for arsenic and antimony was carried out by inductively coupled plasma-mass spectrometry (ICP-MS) (Agilent 7700x, with HMI). Total As and Sb concentrations were measured in the experiments. Through the analysis procedure, quality control and guarantee procedures were implemented. To control the validity of the calibration curve, CCVSS (continuous check verification standard solution) was used.

2.5. Batch Adsorption Tests

To evaluate the efficiency of the adsorbent for arsenic and antimony removal, batch adsorption experiments were performed which included the effect of process variables (i.e., pH, contact time, initial arsenic concentration, and adsorbent dose). Besides that, co-removal of the antimony ions with arsenic was conducted, mixtures of arsenic and antimony solutions with different ratios were prepared; and batch experiments were applied to determine the treatment

performance. Finally, groundwater obtained from the Bayindir-Dernekli well was used in the experiments to demonstrate the interference of the other ions in water.

In the experiments, various dosages of the adsorbent (from 0.05 g to 0.5 g) and 50 mL of arsenic containing water at various initial arsenic concentrations from 50 to 500 μgL^{-1} were put in 250 ml Erlenmeyer flasks. The pH values of the samples were arranged as 3.0, 5.0, 7.0 and 10.0 by putting in 0.1 M sodium hydroxide and hydrochloric acid (Caporale et al., 2013). The data indicated in similar studies were also considered for planning of the batch tests (Arıkan, 2017; Dayton and Basta, 2005; Gibbons and Gagnon, 2010; Makris et al., 2006). After a predetermined contact time, shaking was stopped, and the mixture in each flask was allowed to settle. After settling, samples were filtered with a 0.45 μm filter and prepared for arsenic measurements. Experiments were performed at room temperature ($23^{\circ}\text{C}\pm 2$) and repeated two times, and the mixtures were shaken at 150 rpm for various durations up to eight hours. To investigate the co-removal of antimony and arsenic, solutions including both arsenic and antimony ions were blended at different ratios in order to simulate the existing conditions in the Dernekli well. And, finally, batch experiments were conducted with groundwater to show the interference of the competing ions.

In this study, the equilibrium data were fitted to Freundlich, Langmuir, and Temkin isotherms. The adsorbent dosages varied between 1-10 gL^{-1} while other variables were kept constant. Experiments were performed for a period of 3 h (180 min) at a speed of 150 rpm. The data were respectively fitted by the Langmuir model (Eq.1), the Freundlich model (Eq. 2), and the Temkin model (Eq. 3).

$$q_e = \frac{q_m b C_e}{1 + b C_e} \quad (1)$$

$$q_e = k_f (C_e)^{\frac{1}{n}} \quad (2)$$

$$q_e = \frac{RT}{b_t} \ln(A_t C_e) \quad (3)$$

where q_e (mgg^{-1}) is the quantity of arsenic adsorbed at equilibrium, q_m (mgg^{-1}) is the adsorption capacity, C_e (mgL^{-1}) is the equilibrium concentration, b (Lmg^{-1}) is the Langmuir adsorption energy, k_f (mgg^{-1}) is the Freundlich adsorption capacity, and n is the affinity coefficient. A_t (Lg^{-1}) is the Temkin equilibrium binding constant, b_t (Jmol^{-1}) is the Temkin isotherm constant, R ($8.314 \text{ Jmol}^{-1} \text{K}^{-1}$) is the universal gas constant, and T (K) is the temperature.

To investigate the kinetic parameters for As (T) adsorption on ZOC-DWTS, the data obtained from analyses were examined using the various kinetic models given below labeled first order, second order, pseudo-first order, and pseudo-second order models. Experiments were carried out for three different initial arsenic concentrations (45.40, 107.50, and 515.20 μgL^{-1}).

2.6. Column Studies

The experiments were carried out using Plexiglas columns with a 1.7 cm internal diameter and an 80 cm length. The columns were filled with ZOC-DWTS, and, to hold the adsorbents, a strainer was placed at the bottom. The flow rate was adjusted by using a peristaltic pump (Thermo Fh100m). To start up, the columns were first filled with media and then backwashed with tap water until the effluent was colorless. Afterwards, the columns were operated with distilled water until the stable media height was obtained. The columns were operated in down-flow mode (Razali et al., 2007) at a 5 mLmin^{-1} flow rate. The adsorbate concentrations used in the study were chosen as 40 μgAsL^{-1} and 80 μgSbL^{-1} considering the actual concentrations of these ions in ground water in the region (i.e., Izmir). Utilization of the initial adsorbate concentrations similar to the existing conditions makes that the results comparable and practically applicable. The pH of the solution was three-determined in previous batch experiments. In the experiments, the effects of the bed height of the adsorbent on the column performance were analyzed while other variables kept constant. The water from the outlet were collected at different intervals and measured for the residual arsenic and antimony in order to determine the breakthrough and exhaustion volume.

During the experiments, exhausted media were regenerated by 1% NaOH solutions. For regeneration, NaOH solution was fed with the 5 mlmin^{-1} flow rate in down-flow mode, and samples were taken from outlet of the column at certain time periods, and arsenic, antimony, and iron measurements were taken. The feeding of the NaOH solution was stopped when the effluent arsenic concentration decreased to the standards by the Turkish minister of health (i.e., 10 μgL^{-1}).

2.7. Modeling of Fixed-Bed Adsorption

Development of the mathematical models is required to predict the breakthrough behavior and the performance of the fixed-bed column. Since defining the adsorption performance experimentally at different conditions (i.e., adsorbate concentrations, adsorbents, etc) takes too much time, mathematical models have been put forward to describe the process and determine the impacts of the predicted parameters on adsorption (Xu et al., 2013). Numerous mathematical models have been developed to evaluate the feasibility and efficiency of column models. The Thomas, Bohart &

Adams, Yoon-Nelson, Clark, Wolborska, and Modified Dose-Response models are the most widely used to analyze the column behavior of adsorbent-adsorbate systems. In this study, Thomas and the Yoon-Nelson model that are widely used mathematical models were evaluated in order to describe breakthrough curves for arsenic and antimony adsorption by ZOC-DWTS. The Thomas model has been widely used in the literature to predict the arsenic adsorption in fixed bed column studies (Chaudhry et. al., 2017; Brion-Roby et al., 2018). It is based on second-order reaction kinetics and is suitable for a adsorption system where external and internal diffusion limitations are invalid (Chaudhry et. al., 2017). In this study, due to its simplicity, compatibility with pseudo-second-order reaction kinetics, and other assumptions, the Thomas model was applied to define the dynamic behavior of the ZOC-DWTS column. The Yoon-Nelson model is an another interesting model for column experiments. The basic hypothesis of this model is that the decreasing rate of adsorption is directly proportional to the adsorbate adsorption and the breakthrough point on the adsorbent. Furthermore, it does not focus on the properties of the adsorbate, the type of adsorbent, and the physical properties of the column bed. Therefore, since Yoon and Nelson model is less complexed than other models and requires no detailed data, it was also applied to describe the adsorption process.

2.7.1. Thomas model

The Thomas model is widely used to describe the fixed-bed column performance (Ghribi and Chlendi, 2011; Rozada et al., 2007). Its behaviour is compatible with the Langmuir isotherm and pseudo-second-order reaction kinetics. Thomas equation can be given as

$$\frac{C_t}{C_0} = \frac{1}{1 + \exp\left(\frac{k_{Th} \cdot q_0 \cdot M}{Q} - k_{Th} \cdot C_0 \cdot t\right)} \quad (4)$$

where C_t (mgL^{-1}) is the effluent concentration at a specific time C_0 (mgL^{-1}) is the influent concentration, K_{Th} ($\text{Lmin}^{-1}\text{mg}^{-1}$) is the Thomas rate constant, q_0 (mgg^{-1}) is the equilibrium uptake per gram of the adsorbent, M (g) is the amount of adsorbent in the column, t (min) is the time, and Q (Lmin^{-1}) is the flowrate when $\ln(C_0/C_t)$ is plot vs time (t), K_{Th} and q_0 can be defined at a specific flow rate using linear regression.

2.7.2. Yoon-Nelson model

The model, which is considered to be a simple theoretical model since less column data is required to construct the model, was used to explore the breakthrough character of the arsenic and antimony adsorption on ZOC-DWTS. The Yoon-Nelson model is expressed as;

$$\frac{\ln C_t}{C_0 - C_t} = K_{YN}t - \frac{t_1}{2}K_{YN} \quad (5)$$

By plotting $\ln C_t/(C_0 - C_t)$ vs time, K_{YN} and $t_{1/2}$ are calculated.

3. Findings and Discussion

3.1. Adsorbent Characterization

The surface morphology of the ZOC-DWTS was analyzed by SEM. SEM images are presented in Fig. 1 at 1000x magnifications. Formation of the zirconium oxide was observed in the ZOC-DWTS images. Herein, more porous and non-homogeneous structure was attributed to the zirconium oxide coating. That these irregular structures improved because of the coating was owing to the amorphous Zr oxide. The surface area increased from $149 \text{ m}^2\text{g}^{-1}$ to $156 \text{ m}^2\text{g}^{-1}$ for materials grain size $< 250 \mu\text{m}$ due to the Zr oxide particles on the surface.

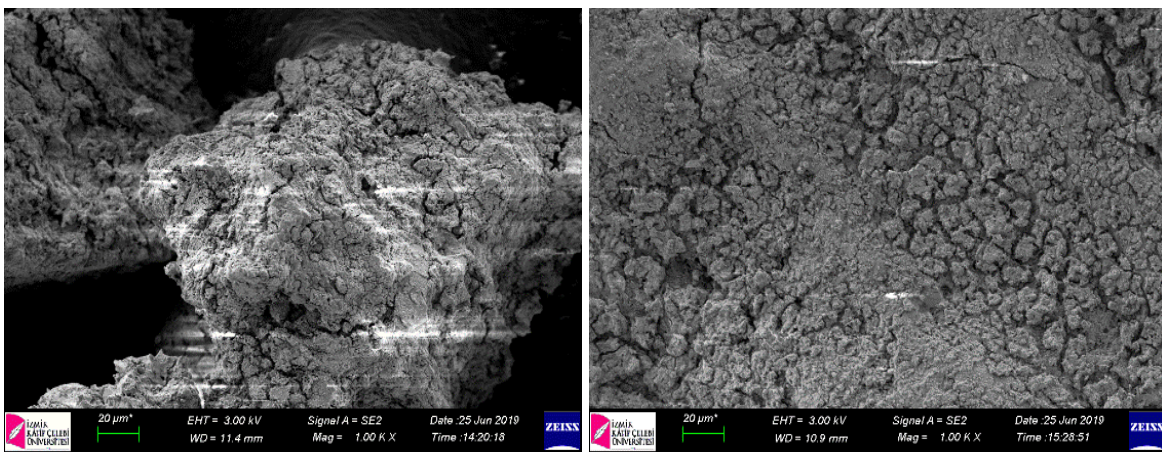


Figure 1. SEM images of ZOC-DWTS

The elemental compositions on the surface of adsorbent were realized by qualitative EDS analysis. The major components were Fe (38.02% for powder and 32.74% for granular),

O (28.69% for powder and 38.32% for granular), Zr (15.1% for powder and 11.93% for granular), and Ca (10.01% for powder and 6.29% for granular). Because EDS analysis focuses on a phase randomly, the results may not express the exact percentages, but it does provide an idea of elemental distribution. Ocinski et al. (2016) found similar results indicating the high content of iron and oxygen in residuals produced from the removal process of iron and manganese of filtration water. The superior content of oxygen might explain their existence in the oxide and oxo-hydroxide form.

Phase analysis of the materials was identified by XRD analysis, and the results are presented in Fig.2. Regarding the XRD analysis, the main phase was mostly iron compounds, calcite, oxygen, and quartz. A zirconium phase was not detected, verifying that $ZrOCl_2 \cdot 8H_2O$ coated only on the surface of the material.

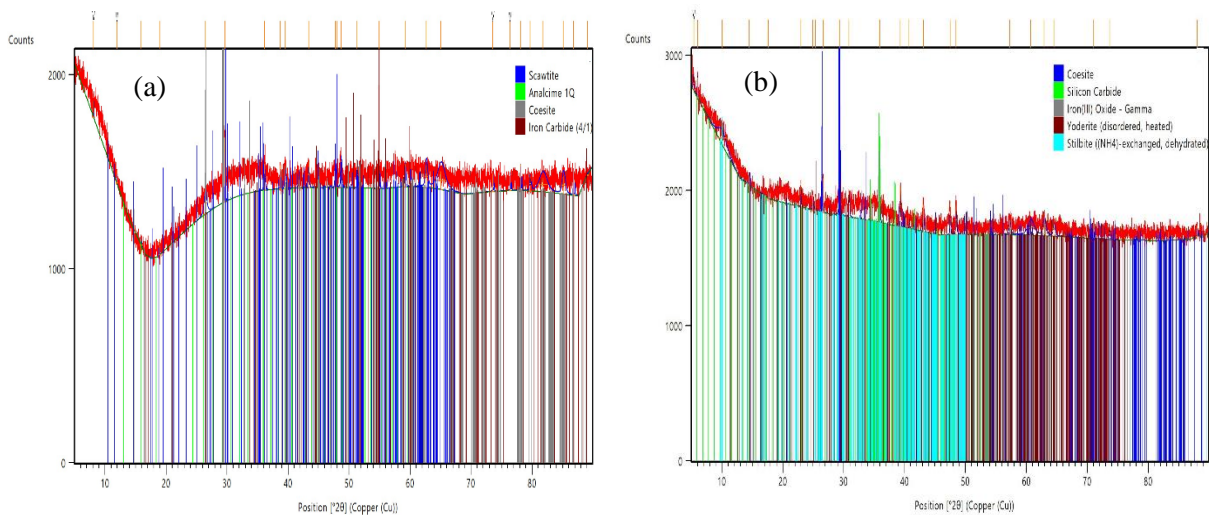


Figure 2. XRD pattern of ZOC-DWTS (a) grain size < 250 μm and (b) grain size: 700 μm , 2 mm

The pore volume and surface area of ZOC-DWTS were assigned by BET analysis. For the powder form, coating with zirconium oxide resulted in an increase in the surface area ($156 \text{ m}^2\text{g}^{-1}$). For the granule form, no significant change was observed. The micropore volume increased from $0.0038 \text{ cm}^3\text{g}^{-1}$ to $0.00634 \text{ cm}^3\text{g}^{-1}$ when DWTS was coated with zirconium. Ocinski et al. (2016) reported that residuals in the drinking water treatment plant had a high surface area (i.e., $120 \text{ m}^2\text{g}^{-1}$). Wang et al. (2016) reported that oxygen-limited heat treatment was resulted in an improvement in the surface area. Surface area of the DWTS after treatment increased from 72.7 to 148-184 m^2g^{-1} . Sidhu et al. (2021) performed metals (Cu, Zn and Pb) and phosphorus removal with wood mulch coated with iron-based water treatment residuals in their study. Coated mulch performed better than uncoated mulch for all pollutants. 21% to

25% higher reductions were observed for metals and 8% higher reduction for P using coated mulch relative to uncoated mulch.

3.2. Batch Experiments

3.2.1. Determination of the Operational Parameters

The surface load of the materials affects the adsorption process and depends on the pH value of the emulsion (Chaudhry et al., 2017). The tests were carried out at different pH values (i.e., pH 3-10). The maximum As (T) removal efficiency (i.e., 99.1%) was obtained at a pH of 3 for ZOC-DWTS. The removal rate reduced with increasing pH values, and an approximately 75.7% efficiency was obtained when pH was at 10. The increase in the As(T) uptake for ZOC-DWTS material may be explained by the increase in the positive surface charges and the synergetic effect of bi-metal oxide (Fe and Zr). The surface load becomes more electronegative when pH values are greater than 7.0, resulting in the decrease of As adsorption onto the material. Similar results were stated by Ocinski et al. (2016) in that acidic conditions (i.e., less than pH 4) favored removal efficiency, and treatment performance reached almost 100%. However, treatment performance was reduced to 70% with increasing pH values.

Contact time (or reaction time) is an important parameter in batch experiments; therefore, the optimum contact was investigated in our study. Approximately 71% of arsenic was removed within 30 minutes, and at the end of two hours, 90% of the arsenic was removed. The equilibrium concentration did not change substantially after 180 minutes, which is when adsorption reached equilibrium.

The optimal adsorbent dosage was investigated by agitating one 10 gL⁻¹ dose of adsorbents in a 50 µgL⁻¹ arsenic solution. The effective dose for ZOC-DWTS was 1 gL⁻¹ to obtain the desired arsenic levels for a 50 µgL⁻¹ initial arsenic concentration (99.5% of arsenic removal was attained).

3.2.2. Adsorption Kinetic Studies

The mechanism and efficiency of the adsorption process are explained by kinetic parameters. The values of adsorption rate constants and the r^2 value, i.e., coefficients of determination, obtained from the linear plots are given in Table 1. The results in Table 1

indicated that the pseudo-second order model ($R^2 \geq 0.999$) provided a better fit to the experimental equilibrium data for As removal by ZOC-DWTS, and adsorption was achieved through the chemical interactive relationship. In addition, correlation coefficients were high, and good agreement was detected between the models and the experimentally equilibrium adsorption capacity value. Chaudhry et al. (2017), Lu et al. (2015), Nekhunguni et al. (2017) and Ren et al. (2014) reported similar results for arsenic sorption onto modified montmorillonite, Zn/Fe layered double hydroxide, iron-zirconium binary oxide-coated sand, and iron (hydr) oxide modified zeolite, respectively.

Table 1. Arsenic adsorption kinetic parameters by ZOC-DWTS

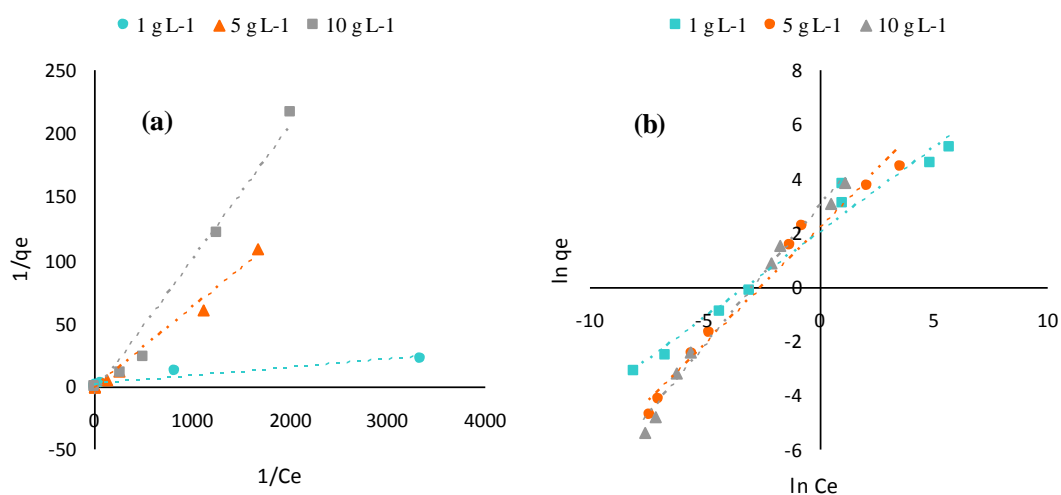
Conc.	$q_{e,exp}$	First order		Pseudo-firstorder			Second order		Pseudo-secondorder		
		k_1	R^2	kp_1	q_e	R^2	k_2	R^2	kp_2	q_e	R^2
μgL^{-1}	mgg^{-1}	min^{-1}		min^{-1}	mgg^{-1}		$\text{Lmg}^{-1}\text{min}^{-1}$		$\text{gmg}^{-1}\text{min}^{-1}$	mgg^{-1}	
45.40	0.042	0.314	0.715	1.419	0.029	0.918	0.059	0.980	111.607	0.045	1.000
107.5	0.104	0.345	0.840	1.215	0.059	0.804	0.031	0.954	30.03	0.107	0.999
515.2	0.486	0.322	0.931	1.040	0.367	0.968	0.004	0.962	2.8409	0.522	0.999

3.2.3. Adsorption Isotherm Studies

Adsorption is mostly defined via isotherms, that is, functions that attribute the quantity of adsorbate to the adsorbent (Desta, 2013). The modeling results given in Table 2 show that the Freundlich model could fit the data better than others with relatively higher R^2 values ($R^2 > 0.97$). Thus, the adsorption is probably multilayer type adsorption according to the Freundlich isotherm theory. The adsorption isotherms (Langmuir and Freundlich) are illustrated in Fig.3; since the Temkin isotherm has very low R^2 values, the figure is not shown. As shown in Fig. 3, ZOC-DWTS showed a high adsorption capacity for arsenic. The K_f values of arsenic were determined to range from 7.380 mgg^{-1} - 18.470 mgg^{-1} for ZOC-DWTS as designated by the Freundlich model. These values were better than that of the predominantly reported adsorbents (Arıkan, 2016; Gibbons and Gagnon, 2010; Chaudhry et al., 2017; Nekhunguni et al., 2017; Ocinskiet al., 2016).

Table 2. The constants of the Langmuir, Freundlich, and Temkin isotherms for the arsenic adsorption on ZOC-DWTS

Dose (g L ⁻¹)	Langmuir			Freundlich			Temkin		
	Q _{max} (mg g ⁻¹)	b (L mg ⁻¹)	R ²	1/n	k _f (mg g ⁻¹)	R ²	A _T (L g ⁻¹)	bt (kJ mol ⁻¹)	R ²
1	0.842	182.000	0.913	0.620	7.380	0.972	0.196	0.243	0.726
5	0.722	22.200	0.991	0.850	8.360	0.980	0.242	0.390	0.703
10	0.137	68.500	0.979	1.030	18.470	0.989	0.435	0.643	0.627

**Figure 3.** Adsorption isotherms of arsenic on ZOC-DWTS (a) Langmuir isotherm, (b) Freundlich isotherm (Empirical conditions: arsenic concentration= 0.047-470 mg L⁻¹, adsorbent dosages= 1, 5, and 10 g L⁻¹, T=25±0.5°C, pH=3)

3.2.4. Co-removal of Arsenic and Antimony Ions

As mentioned above, experiments were performed with varying As/Sb concentrations in order to determine the optimum As/Sb ratio. The mixtures were (1) 35 µg AsL⁻¹ + 35 µg SbL⁻¹, (2) 90 µg AsL⁻¹ + 90 µg SbL⁻¹, (3) 35 µg AsL⁻¹ + 90 µg SbL⁻¹, and (4) 90 µg AsL⁻¹ + 35 µg SbL⁻¹. The results showed that almost 99% of As could be successfully removed from water. Moreover, As removals were not affected by Sb concentrations, and the adsorbent (i.e., ZOC-DWTS) could efficiently remove the As. The ZOC-DWTS was capable of sorbing more than 85% of Sb. Similar to As removal, efficiency was not affected by the As/Sb ratios.

3.2.5. Effect of Existing Ions in Groundwater on Adsorption

Groundwater sample collected from the Bayindir/Izmir region was used to show the interference of the other ions with arsenic adsorption. Batch studies were carried out in the presence of certain anions and cations found in real ground water samples. 1 g ZOC-DWTS L⁻¹ was dosed at pH 3 at 25°C in the experiments. Fe, Mn, As, and Sb concentrations in raw water were measured as 300 µg L⁻¹, 269 µg L⁻¹, 9 µg L⁻¹, and 56 µg L⁻¹, respectively. The phosphate concentration was around 4 mg L⁻¹. After adsorption, concentration of the arsenic ions reduced to about 1 µg L⁻¹, yielding 90% efficiency. Antimony concentration decreased to 17 µg L⁻¹, which were not sufficient to fulfill the standards. Similar to arsenic and antimony, Fe also decreased from 300 µg L⁻¹ to 14 µg L⁻¹. Only the manganese concentrations increased, reaching 670 µg L⁻¹. Herein, the increase in the Mn concentration following adsorption was explained by it being released from the sludge under acidic condition. The results gathered from experiments with real groundwater samples showed that the ions have an impact on the treatment performance on ZOC-DWTS.

The existence of competing anions resulted in a decrease in arsenic and antimony removal efficiencies by approximately 10% for arsenic and 15% for antimony, compared to synthetic water. Li et al. (2012) and Nekhunguni et al. (2017) indicated that phosphate ions (PO₄³⁻) had an inhibitory effect on arsenic and antimony removal at high concentrations. In this study, the impacts of phosphate ions were negligible because influent concentration was lower than 0.4 mg L⁻¹.

3.3. Column Studies

The column experiments were performed with synthetic water containing 40 µg L⁻¹ of arsenic and 80 µg L⁻¹ of antimony. The pH of the solution was set to 3 and then pumped into the column at a 5 mL min⁻¹ flow rate. The empty bed contact time was determined to be 4.54 min for a 10 cm bed depth and 9.04 min for a 20 cm bed depth. The arsenic and antimony guideline concentrations for drinking water (i.e., 10 µg L⁻¹ for As and 5 µg L⁻¹ for Sb) were defined as the breakthrough point. The breakthrough curves acquired for arsenic and antimony removal on ZOC-DWTS at a 5 mL min⁻¹ flow rate, and two different bed depths are indicated in Fig. 4. The breakthrough curves exhibited a typical S-shape, as anticipated in this study. As depicted by Fig. 4, the breakthrough volumes altered with bed depth. The breakthrough volume increased with increasing bed depth because there were further binding sites for

adsorption. The rise in adsorbent dosages in the higher beds, which supplied larger adsorption regions for arsenic, provided the rise in contaminant removal with bed depth. Conversely, because the arsenic ions did not have sufficient time to adsorb onto ZOC-DWTS at lower bed depth, a decrease in the breakthrough was achieved.

In the experiments, the breakthrough volume increased from 4420 L (195000 BV) to 7444 L (165000 BV) with an increasing bed depth from 10 to 20 cm for arsenic. Similarly, the column exhaustion volume increased with the increase in bed depth. Exhausted volumes raised from 8020 L and 13780 L for the 10 and 20 cm of bed depths. The results for the ZOC-DWTS were better than those achieved by Pal (2001) and Gibbons and Gagnon (2010). Pal (2001) used GFH for arsenic removal. The desired arsenic concentration (i.e., $10 \mu\text{g L}^{-1}$) was obtained at a 60000-bed volume (BV), which were lower than this study.

Breakthrough curves for antimony removal at different bed depths are also shown in Fig. 4. For antimony adsorption, ZOC-DWTS achieved antimony removal of 22000 and 18000 bed volumes for 20 cm and 10 cm bed depths, respectively. Then, antimony concentrations rose above $5 \mu\text{g SbL}^{-1}$. Similarly, exhausted volumes increased from 3412 L to 6004 L, with increasing depths. Therefore, the results revealed that increasing bed depth caused more active adsorption sites, providing additional treated volume until the exhaustion point. Ilavsky (2008) used the Bayoxide E33 and GEH for the removal of antimony for 62.50 and 65.10 $\mu\text{g L}^{-1}$ initial concentrations and found that the GEH adsorbent is more efficient (1288 bed volume) for antimony removal in regard to Bayoxide E33. However, in this study, ZOC-DWTS were reached breakthrough point after 22000 bed volumes at a bed depth of 20 cm and was thus found to be more effective than GEH and Bayoxide E33.

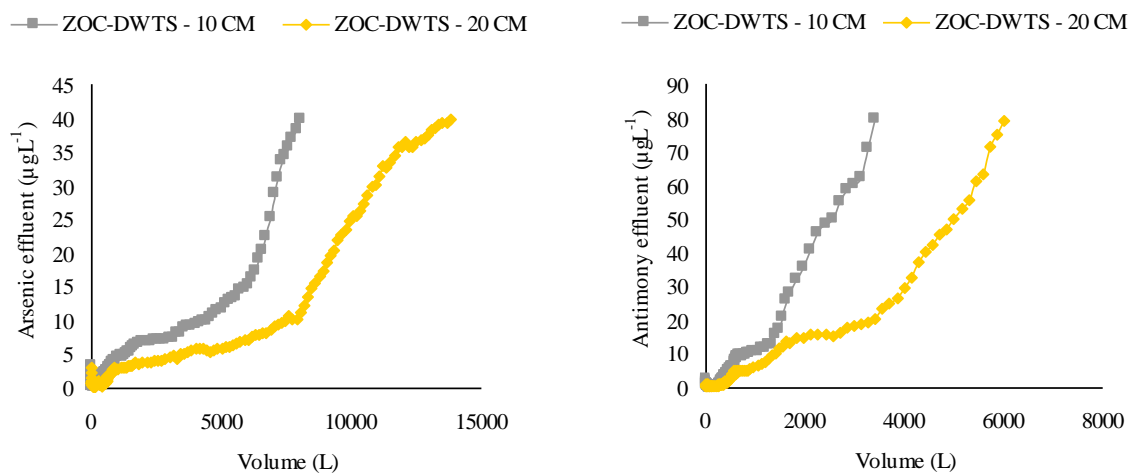


Figure 4. Breakthrough curves for arsenic and antimony removal at different bed depth

3.4. Modeling of Fixed-Bed Adsorption

3.4.1. Thomas model

The values of the model parameters on arsenic and antimony for ZOC-DWTS, i.e., K_{Th} and q_0 are presented in Table 3. These values illustrate that the Thomas model fitted to the empirical data well, and R^2 values ranged from 0.80 to 0.92 for arsenic and 0.83 to 0.88 for antimony on ZOC-DWTS.

The maximum adsorption capacity (q_0) increased when the bed depths increased, except for antimony. In addition, the Thomas rate constant, k_{Th} , decreased with increasing bed depths. Kundu and Gupta (2007) found similar findings which q_0 decreased with increasing bed depths. However, the q_0 values (i.e., 0.14 mgg^{-1} - 0.30 mgg^{-1}) reported by them were noticeably lower than ZOC-DWTS.

The breakthrough curves obtained experimental data and predicted values using the Thomas model at various bed depths on adsorbents are illustrated in Fig. 5 for arsenic and antimony. Fig. 5 shows that the dissimilarities between the model values and experiments were negligible, especially for 20 cm bed depths for arsenic. Thus, higher correlation coefficients were obtained for a higher bed depth of 20 cm except for antimony removal. Adsorption capacities (from 8.74 to 9.13 mgg^{-1}) calculated from the model for arsenic removal were higher than those achieved in Kundu and Gupta (2007) where 0.146 to 0.308 mgg^{-1} adsorption capacity was obtained, even though there were some discrepancies in the experimental setup, particularly adsorbents (iron oxide coated cement vs ZOC-DWTS in this experiment), column geometry, flow mode (up-flow vs down-flow in this study), initial concentration (1.35 mgL^{-1} vs 0.04 mgL^{-1} in this study), and flow rate (8.5 $mlmin^{-1}$ vs 5 $mlmin^{-1}$ in this study).

Table 3. Thomas model parameters for arsenic and antimony adsorption onto ZOC-DWTS at different bed depths

Contaminant	h (cm)	Q($mlmin^{-1}$)	$C_0(mgL^{-1})$	$k_{Th}(Lmin^{-1}mg^{-1})$	$q_0(mgg^{-1})$	R^2
Arsenic	10	5	0.04	0.1	8.74	0.804
	20	5	0.04	0.05	9.13	0.918
Antimony	10	5	0.08	0.125	8.67	0.833
	20	5	0.08	0.075	6.82	0.877

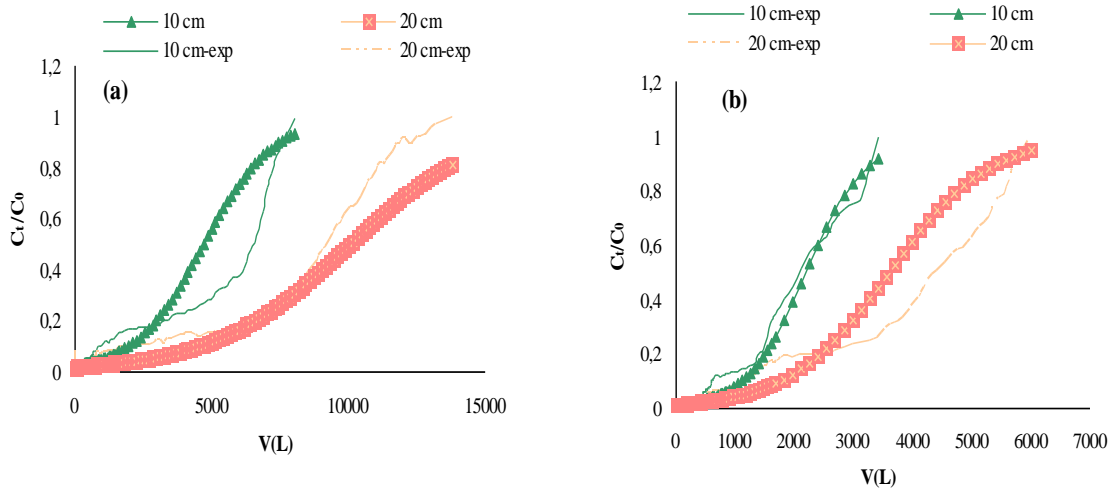


Figure 5. Breakthrough curves obtained from the experiments and the Thomas model for (a) Arsenic and (b) Antimony adsorption onto ZOC-DWTS at different heights ($Q=5 \text{ mlmin}^{-1}$, $C_0(\text{As})= 40 \text{ }\mu\text{gL}^{-1}$, $C_0(\text{Sb})= 80 \text{ }\mu\text{gL}^{-1}$)

3.4.2. Yoon-Nelson model

The values of the model parameters on arsenic and antimony for ZOC-DWTS, i.e., K_{YN} and $t_{1/2}$, were calculated and presented in Table 4. K_{YN} , which is defined by the Yoon-Nelson rate constant, decreased whereas the 50% adsorbate breakthrough time, $t_{1/2}$, and R^2 values increased with increasing bed depths. Breakthrough curves obtained for both experimental data and model values at various bed depths are illustrated in Fig. 6. High correlation coefficients (R^2) which ranged from 0.83 to 0.92 indicated that the empirical data could be well fitted to the Yoon-Nelson model except for the 10 cm bed depth on arsenic ($R^2= 0.80$). Table 4 shows that the correlation coefficient (R^2) of the Yoon-Nelson equation is same as that of the Thomas equation.

Table 4. Yoon-Nelson model parameters for arsenic and antimony adsorption onto ZOC-DWTS at different bed depths

Contaminant	h (cm)	Q (ml min ⁻¹)	C ₀ (mg L ⁻¹)	k _{YN} (min ⁻¹)	t _{1/2} (h)	R ²
Arsenic	10	5	0.04	0.4x10 ⁻⁵	16,478	0.8035
	20	5	0.04	0.2x10 ⁻⁵	34,396	0.9179
Antimony	10	5	0.08	0.1x10 ⁻⁴	8,163	0.8331
	20	5	0.08	0.6x10 ⁻⁵	12,848	0.8766

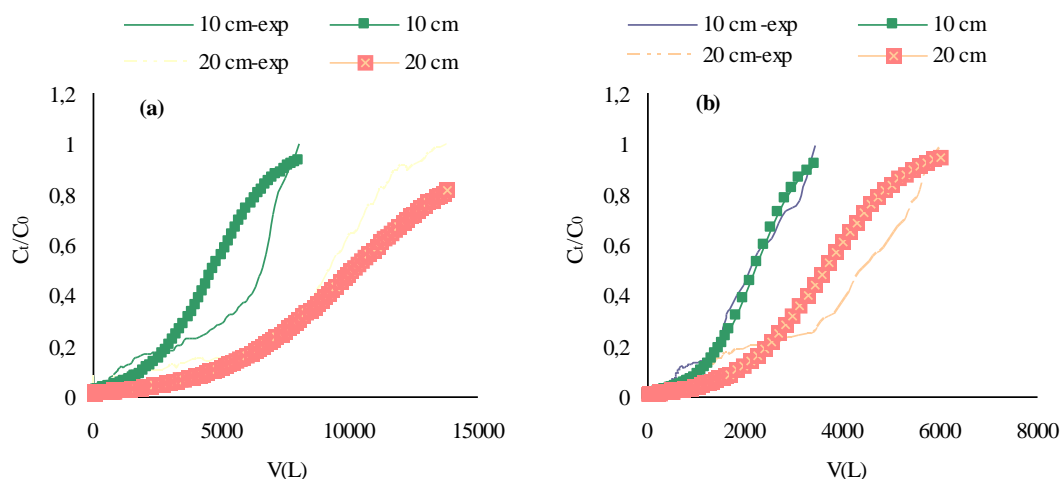


Figure 6. Breakthrough curves obtained from the experiments and the Yoon-Nelson model for (a) Arsenic and (b) Antimony adsorption onto ZOC-DWTS at various bed heights ($Q=5 \text{ mlmin}^{-1}$, $C_0(\text{As})=40 \text{ }\mu\text{gL}^{-1}$, $C_0(\text{Sb})=80 \text{ }\mu\text{gL}^{-1}$)

3.5. Regeneration Studies

Regeneration studies were performed in a 1% sodium hydroxide solution. For regeneration, a NaOH solution was fed with the same flow rate (5 mlmin^{-1}) in down flow mode. Regeneration terminated at the end of the 12 days because both arsenic and antimony concentrations did not decrease the desired level. Besides that, a clogging problem in the column occurred during the regeneration. Therefore, ZOC-DWTS after regeneration were no longer effective for arsenic and antimony removal.

4. Conclusions and Recommendations

The adsorption method was proposed as an appropriate and suitable approach to arsenic and antimony removal in rural areas due to its simplicity and ease of operation and handling, if low-cost and efficient adsorbents are used. Therefore, worldwide studies have been focused on developing more efficient, economic, and sustainable adsorbents to remove metalloids and toxic metals from contaminated waters (e.g., arsenic and antimony). Waste materials for removal of arsenic and other pollutants from water are of great importance because they reduce waste disposal and can be cost-effective. The sludge used in this study was rich in ironoxide and thus exhibited excellent binding properties for arsenic compounds. In addition, coating with zirconium displayed a synergistic effect, and synthesized Fe-Zr binary oxide

exhibited simultaneous removal of arsenic and antimony. Herein, producing the Fe-Zr binary oxide (ZOC-DWTS) from a waste material (i.e., sludge) by using a simple and low-cost process offer advantages in terms of sustainability and economy. An additional advantage was obtained when simultaneous removal of arsenic and antimony below the standards was achieved.

An adsorption isotherm study was carried out on three well known isotherms models, the Langmuir, Freundlich, and Temkin isotherms. The Freundlich model yielded a somewhat better fit ($R^2 > 0.97$). The fitted model indicated that adsorption probably occurs on the surface. Kinetic studies showed that the pseudo-second order model ($R^2 \geq 0.999$) matched perfectly with the experimental data for arsenic removal. Compatibility of the experimental data and model values of the equilibrium adsorption capacity and high correlation coefficients indicated that arsenic adsorption onto ZOC-DWTS followed the pseudo-second order reaction kinetic, and chemical interaction was achieved in the sorption. Column experiments were performed in various conditions to demonstrate the applicability of ZOC-DWTS for arsenic and antimony removal. The experimental results obtained from the column test demonstrated that 7444 L (165000 BV) water was effectively treated below $10 \mu\text{gL}^{-1}$ for arsenic and 820 L (18000 BV) water was treated below $5 \mu\text{gL}^{-1}$ for antimony by ZOC-DWTS. The experimental data from the column study fitted well to the Thomas and Yoon–Nelson models. The dynamic action of the adsorption process was successfully described by both models. The high adsorption capacity of the ZOC-DWTS indicated that the adsorbent could compete with other commercial adsorbents on the market (Table 5).

Table 5. Comparison of the ZOC-DWTS and other adsorbents

Adsorbent	Adsorption capacity (mgg^{-1})	Removal capacity (Bed volume)	Regeneration	References
ZOC-DWTS	9.13 As(T) 8.67 Sb(T)	165000 (As) 18000 (Sb)	not available	This study
DWTS-200	6.53 As(T) 5.21 Sb(T)	133000 (As) 14000 (Sb)	available	Kavacik and Dolgen (unpublished)
Granule iron (III) hydroxide oxide	2.05 As(V) 0.07 As(III) 0.25 Sb(V)	50000-100000 (As)	not available	Kolbe et al. (2011) Driehaus, (2002)
Iron-impregnated activated carbon	43.6-51.3 As(V) 38.8-39.2 As(III)	12000-13000 (As)	-	Chen et al. (2007)
Iron coated seaweeds	4.2 As(III) 7.3 As(V)	-	-	Vieira et al. (2017)

Authors' Contributions

All authors contributed equally to the study.

Statement of Conflicts of Interest

There is no conflict of interest between the authors.

Statement of Research and Publication Ethics

The author declares that this study complies with Research and Publication Ethics.

References

- Arıkan, S. (2016). *Investigation of arsenic adsorption performance of the modified natural materials* (Unpublished Doctoral Dissertation). Graduate School of Natural and Applied Sciences, Dokuz Eylül University, İzmir.
- Arıkan, S., Dolgen, D., and Alpaslan, M.N. (2017). Arsenic removal from aqueous solutions using iron oxide coating sepiolite. *Fresenius Environment Bulletin (FEB)*, 26 (12A), 7634-7642.
- Baba, A., Tayfur, G. (2011). Groundwater contamination and its effect on health in Turkey. *Environ Monit Assess* **183**, 77–94. <https://doi.org/10.1007/s10661-011-1907-z>
- Brion-Roby, R., Gagnon, J., Deschenes, J.S., and Chabot, B. (2018). Development and treatment procedure of arsenic-contaminated water using a new and green chitosan sorbent: Kinetic, isotherm, thermodynamic and dynamic studies. *Pure Appl. Chem.*, 90(1), 63–77.
- Caporale, A.G., Punamiya, P., Pigna, M., Violante, A., and Sarkar, D. (2013). Effect of particle size of drinking water treatment residuals on the sorption of arsenic in the presence of competing ions. *Journal of Hazardous Materials*, 260, 644-651. <http://dx.doi.org/10.1016/j.jhazmat.2013.06.023>
- Chaudhry, S.A., Zaidi, Z., and Siddiqui, S.I. (2017). Isotherm, kinetic and thermodynamics of arsenic adsorption onto Iron-Zirconium Binary Oxide-Coated Sand (IZBOCS): Modelling and process optimization. *Journal of Molecular Liquids*, 229, 230-240. <http://dx.doi.org/10.1016/j.molliq.2016.12.048>
- Chen, W., Parette, R., Zou, J., Cannon, F.S., and Dempsey, B.A. (2007). Arsenic removal by iron-modified activated carbon. *Water Research*, 41, 1851-1858. <http://dx.doi.org/10.1016/j.watres.2007.01.052>
- Chen, B., Zhou, D., and Zhu, I. (2008). Transitional adsorption and partition of nonpolar and polar aromatic contaminants by biochars of pine needles with different pyrolytic temperatures. *Environmental Science Technology*, 42, 5137-5143.
- Chaudhry, S.A., Zaidi, Z., and Siddiqui, S.I. (2017). Isotherm, kinetic and thermodynamics of arsenic adsorption onto Iron-Zirconium Binary Oxide-Coated Sand (IZBOCS): Modelling and process optimization. *Journal of Molecular Liquids*, 229, 230-240.
- Dayton, E.A., and Basta, N.T. (2005). A method for determining the phosphorus sorption capacity and amorphous aluminium of aluminium-based drinking water treatment residuals. *J. Environ. Qual.*, 34, 1112.

- Desta, M.B. (2013). Batch sorption experiments: Langmuir and freundlich isotherm studies for the adsorption of textile metal ions onto teffstraw (Eragrostistef) agricultural waste. *Journal of Thermodynamics*, vol. 2013, Article ID 375830, 6 pages. <https://doi.org/10.1155/2013/375830>.
- Dolgen, D., Kavacik, B., and Alpaslan, M.N. (2019). Emerging options for arsenic removal in remote areas. *International Journal of Environmental Research and Technology*, IJERAT, 2(1) 01-07. E-ISSN, 2667-4041.
- Drieheus, W. (2002). Arsenic removal-experience with the GEH process in Germany. *Water Science and Technology: Water Supply*, 2(2), 275-280.
- Ghribi, A., and Chlendi, M. (2011). Modeling of fixed bed adsorption: Application to the adsorption of organic dye. *Asian Journal of Textile*, 1(4), 161-171.
- Gibbons, M.K., and Gagnon, G.A. (2010). Adsorption of arsenic from a Nova Scotia groundwater onto water treatment residual solids. *Water Research*, 44, 5740-5749. <http://doi.org/10.1016/j.watres.2010.06.050>.
- Ilavsky, J. (2008). Removal of antimony from water by sorption materials. *Slovak Journal of Civil Engineering*, 2008/2, 1-6.
- Ippolito, J.A., Barbarick, K.A., and Elliott, H.A. (2011). Drinking water treatment residuals: A review of recent uses. *Journal of Environmental Quality*, 40(1), 1-12.
- Kavacik, B., and Dolgen, D. (unpublished). Isıl işlem ile modifiye edilmiş arıtma çamuru kullanılarak sabit yataklı kolonda arsenik ve antimon giderimi. *Gazi University Engineering and Architect Faculty Journal*. (Acceptance date: 2022, March)
- Kolbe, F., Weiss, H., Morgenstern, P., Wennrich, R., Lorenz, W., Schurk, K., Stanjek, H., and Daus, B. (2011). Sorption of aqueous antimony and arsenic species onto akagenite. *Journal of Colloid and Interface Science*, 357, 460-465. <http://doi.org/10.1016/j.jcis.2011.01.095>.
- Kumar, A., Ali, M., Kumar, R., Kumar, M., Sagar, P., Pandey, R.K., Akhouri, V., Kumar, V., Anand, G., Niraj, P.K., Rani, R., Kumar, S., Kumar, D., Bishwapriya, A., and Ghosh, A.K. (2021). Arsenic exposure in Indo Gangetic plains of Bihar causing increased cancer risk. *Scientific Reports*, 11, 2376.
- Kundu, S., and Gupta, A.K. (2007). As(III) removal from aqueous medium in fixed bed using iron oxide-coated cement (IOCC): Experimental and modeling studies. *Chemical Engineering Journal*, 129, 123-131. <http://doi.org/10.1016/j.cej.2006.10.014>.
- Lan, B., Wang, Y., Wang, X., Zhou, X., Kang, Y., and Li, L. (2016). Aqueous arsenic (As) and antimony (Sb) removal by potassium ferrate. *Chemical Engineering Journal*, 292, 389-397. <http://dx.doi.org/10.1016/j.cej.2016.02.019>.
- Lee, S.H., Tanaka, M., Takahashi, Y., and Kim, K.W. (2018). Enhanced adsorption of arsenate and antimonate by calcined Mg/Al layered double hydroxide: Investigation of comparative adsorption mechanism by surface characterization. *Chemosphere*, 211, 903-911. <https://doi.org/10.1016/j.chemosphere.2018.07.153>.
- Li, X.H., Dou, X.M., and Li, J.Q. (2012). Antimony (V) removal from water by iron-zirconium bimetal oxide: performance and mechanism. *J. Environ. Sci. China*, 24(7), 1197-1203. [https://doi.org/10.1016/S1001-0742\(11\)60932-7](https://doi.org/10.1016/S1001-0742(11)60932-7)
- Li, F., Cao, X., Zhao, I., Wang, J., and Ding, Z. (2014). Effects of mineral additives on biochar formation: carbon retention, stability and properties. *Environmental Science Technology*, 48, 11211-11217.
- Lu, H., Zhu, Z., Zhang, H., Zhu, J., and Qiu, Y. (2015). Simultaneous removal of arsenate and antimonate in simulated and practical water samples by adsorption onto Zn/Fe layered double hydroxide. *Chemical Engineering Journal*, 276, 365-375. <http://dx.doi.org/10.1016/j.cej.2015.04.095>.
- Long, X., Wang, T., He, M. (2022). Simultaneous removal of antimony and arsenic by nano-TiO₂-crosslinked chitosan (TA-chitosan) beads, *Environmental Technology*, DOI:10.1080/09593330.2022.2048084
- Makris, K.C., Sarkar, D., and Datta, R. (2006). Evaluating a drinking water waste by-product as a novel sorbent for arsenic. *Chemosphere*, 64, 730-741. <http://doi.org/10.1016/j.chemosphere.2005.11.054>.

- Masue, Y., Loeppert, R.H., and Kramer, T.A. (2006). Arsenate and arsenite adsorption and desorption behavior on coprecipitated aluminum: iron hydroxides. *Environmental Science & Technology*, 41(3), 837-843.
- Nagar, R., Sarkar, D., Makris, K.C., and Data, R. (2010). Effect of solution chemistry on arsenic sorption by Fe- and Al-based drinking-water treatment residuals. *Chemosphere*, 78(8), 1028-1035. <http://doi.org/10.1016/j.chemosphere.2009.11.034>.
- Nekhunguni, P.M., Tavengwa, N.T., and Tutu, H. (2017). Investigation of As(V) removal from acid mine drainage by iron (hydr) oxide modified zeolite. *Journal of Environmental Management*, 197, 550-558. <http://dx.doi.org/10.1016/j.jenvman.2017.04.038>.
- Ocinski, D., Jacukowicz-Sobala, I., Mazur, P., Raczek, J., and Kociolek-Balawejder, E. (2016). Water treatment residuals containing iron and manganese oxides for arsenic removal from water: characterization of physicochemical properties and adsorption studies. *Chemical Engineering Journal*, 294, 210-221. <http://dx.doi.org/10.1016/j.cej.2016.02.111>.
- Pal, B.N. (2001). Granular ferric hydroxide for elimination of arsenic from drinking water. Technologies for Removal of Arsenic from Drinking Water. <https://archive.unu.edu/env/Arsenic/Pal.pdf>. Accessed 03 February 2021.
- Razali, M., Zhao, Y.Q., and Bruen, M. (2007). Effectiveness of a drinking water treatment sludge in removing different phosphorus species from aqueous solution. *Separation and Purification Technology*, 55, 300-306. <http://doi.org/10.1016/j.seppur.2006.12.004>.
- Ren, X., Zhang, Z., Luo, H., Hu, B., Dang, Z., Yang, C., and Li, L. (2014). Adsorption of arsenic on modified montmorillonite. *Appl. Clay Sci.* 97, 17-23. <http://dx.doi.org/10.1016/j.clay.2014.05.028>.
- Rozada, F., Otero, M., Garcia, A.I., and Moran, A. (2007). Application in fixed bed systems of adsorbents obtained from sewage sludge and discharged tyres. *Dyes Pigm.* 72, 47-56.
- Sasaki, T., Iizuka, A., Watanabe, M., Hongo, T., and Yamasaki, A. (2014). Preparation and performance of arsenate (V) adsorbents derived from concrete wastes. *Waste Management*, 34(10), 1829-1835. <http://dx.doi.org/10.1016/j.wasman.2014.01.001>.
- Shajia, M., Santosh, M., Sarath, K.V., Prakash, P., Deepchand, B., and Divyaa, B.V. (2021). Arsenic contamination of groundwater: A global synopsis with focus on the Indian Peninsula. *Geoscience Frontiers*, 12, 101079.
- Shtangeeva, I., Bali, R., and Harris, A. (2011). Bioavailability and toxicity of antimony. *Journal of Geochemical Exploration*, 110, 40-45.
- Sidhu, V., Barrett, K., Park, D.Y., Deng, Y., Datta, R., and Sarkar D. (2021). Wood mulch coated with iron-based water treatment residuals for the abatement of metals and phosphorus in simulated stormwater runoff. *Environmental Technology & Innovation*, 21, 101214. <https://doi.org/10.1016/j.eti.2020.101214>.
- Soleimanifar, H., Deng, Y., Wu, L., and Sarkar, D. (2016). Water treatment residual (WTR)-coated wood mulch for alleviation of toxic metals and phosphorus from polluted urban stormwater runoff. *Chemosphere*, 154, 289-292.
- Sun, J., Pikaar, I., Sharma, K.R., Keller, J., and Yuan, Z. (2015). Feasibility of sulfide control in sewers by reuse of iron rich drinking water treatment sludge. *Water Research*, 71, 150-159. <http://dx.doi.org/10.1016/j.watres.2014.12.044>.
- Tan, G., Wu, Y., Liu, Y., & Xiao, D. (2018). Removal of Pb(II) ions from aqueous solution by manganese oxide coated rice straw biochar – A low-cost and highly effective sorbent. *Journal of the Taiwan Institute of Chemical Engineers*, 84, 85-92.
- Wang, C., Jiang, H., Yuan, N., Pei, Y., and Yan, Z. (2016). Tuning the adsorptive properties of drinking water treatment residue via oxygen-limited heat treatment for environmental recycle. *Chemical Engineering Journal*, 284, 571-581. <http://dx.doi.org/10.1016/j.cej.2015.09.011>.
- Wang, C., Wu, Y., Bai, L., Zhao, Y., Yan, Z., Jiang, H., and Liu, X. (2018). Recycling of drinking water treatment residue as an additional medium in columns for effective P removal from eutrophic surface water. *Journal of Environmental Management*, 217, 363-372. <http://doi.org/10.1016/j.jenvman.2018.03.128>.

- WHO/SDE/WSH, 2003. Antimony in drinking-water. Background document for development of WHO guidelines for drinking-water quality. Retrieved from https://www.who.int/water_sanitation_health/dwq/chemicals/antimony.pdf
- Xi, J., He, M., and Lin, C. (2010). Adsorption of antimony(V) on kaolinite as a function of pH, ionic strength and humic acid. *Environ Earth Sci.*, 60, 715–722.
- Xu, Z., Cai, J., and Pan, B. (2013). Mathematically modeling fixed-bed adsorption in aqueous systems. *Journal of Zhejiang University-SCIENCE A (Applied Physics & Engineering)*, 14(3), 155-176.
- Varol, S., Köse, İ. (2018). Effect on human health of the arsenic pollution and hydrogeochemistry of the Yazır Lake wetland (Çavdır-Burdur/Turkey). *Environ Sci Pollut Res* **25**, 16217–16235. <https://doi.org/10.1007/s11356-018-1815-7>
- Vieira, B.R.C., Pintor, A.M.A., Boaventura, R.A.R., Botelho, C.M.S. (2017). Arsenic removal from water using iron-coated seaweeds. *Journal of Environmental Management*, 192, 224-233. <http://dx.doi.org/10.1016/j.jenvman.2017.01.054>.
- Zhang, G.S., Qu, J.H., Liu, H.J., Liu, P.R., and Wu, R.C. (2007). Preparation and evaluation of a novel Fe-Mn binary oxide adsorbent for effective arsenite removal. *Water Res.*, 41, 1921-1928. <http://doi.org/10.1016/j.watres.2007.02.009>.